Received: 29 June 2023 | Revised: 18 September 2023 | Accepted: 29 October 2023

DOI: 10.1002/yea.3908

RESEARCH ARTICLE

Yeast WILEY

MKT1 alleles regulate stress responses through posttranscriptional modulation of Puf3 targets in budding yeast

Koppisetty Viswa Chaithanya[1,2] | Himanshu Sinha[1,2,3]

[1]Department of Biotechnology, Bhupat and Jyoti Mehta School of Biosciences, IIT Madras, Chennai, Tamil Nadu, India

[2]Centre for Integrative Biology and Systems Medicine (IBSE), IIT Madras, Chennai, Tamil Nadu, India

[3]Robert Bosch Centre for Data Science and Artificial Intelligence (RBCDSAI), IIT Madras, Chennai, Tamil Nadu, India

Correspondence
Himanshu Sinha, Department of Biotechnology, Bhupat and Jyoti Mehta School of Biosciences, IIT Madras, Chennai 600036, Tamil Nadu, India.
Email: sinha@iitm.ac.in

Funding information
Indian Institute of Technology Madras; Excelra Knowledge Solutions Pvt. Ltd.; University Grants Commission

Abstract

MKT1 is a pleiotropic stress response gene identified by several quantitative trait studies with *MKT1*^{89G} as a causal variant, contributing to growth advantage in multiple stress environments. *MKT1* has been shown to regulate *HO* endonuclease posttranscriptionally via the Pbp1–Pab1 complex. RNA-binding protein Puf3 modulates a set of nuclear-encoded mitochondrial transcripts whose expression was found to be affected by *MKT1* alleles. This study attempts to relate the *MKT1* allele-derived growth advantage with the stability of Puf3 targets during stress and elucidate the roles of Pbp1 and Puf3 in this mechanism. Our results showed that the growth advantage of the *MKT1*^{89G} allele in cycloheximide and H_2O_2 was *PBP1*-dependent, whereas in 4-nitroquinoline 1-oxide, the growth advantage was dependent on both *PUF3* and *PBP1*. We compared the messenger RNA decay kinetics of a set of Puf3 targets in multiple stress environments to understand the allele-specific regulation by *MKT1*. In oxidative stress, the *MKT1*^{89G} allele modulated the differential expression of nuclear-encoded mitochondrial genes in a *PBP1*- and *PUF3*-dependent manner. Additionally, *MKT1*^{89G} stabilised Puf3 targets, namely, *COX17*, *MRS1* and *RDL2*, in an allele and stress-specific manner. Our results showed that *COX17*, *MRS1* and *RDL2* had a stress-specific response in stress environments, with the *MKT1*^{89G} allele contributing to better growth; this response was both *PBP1*- and *PUF3*-dependent. Our results indicate that the common allele, *MKT1*^{89G}, regulates stress responses by differentially stabilising Puf3-target mitochondrial genes, which allows for the strain's better growth in stress environments.

KEYWORDS

MKT1, oxidative stress response, posttranscriptional regulation, QTL, RNA-binding proteins

1 | INTRODUCTION

The environment, with its dynamic compositional changes, poses a consistent threat to the cellular homeostatic balance (Simpson & Ashe, 2012). Cells display an array of survival mechanisms to deal with these fluctuations by deploying environmental stress response (ESR), where the normal physiological course is transiently substituted with the synthesis of ESR-associated proteins (Buchan & Parker, 2009; Buchan et al., 2011; Causton et al., 2001; Lackner et al., 2012; Loll-Krippleber & Brown, 2017). Cellular regulation of gene expression during stress conditions predominantly employs posttranscriptional and translational controls to modulate their synthetic activity (Lackner et al., 2012; Martínez-Salas et al., 2013).

 © 2023 John Wiley & Sons Ltd.

RNA-binding proteins associated with specific transcripts post-transcriptionally regulate their expression by modulating their localisation, degradation and translation (Gupta et al., 2014; Kechavarzi & Janga, 2014; Martínez-Salas et al., 2013; Saint-Georges et al., 2008). Members of the Pumilio-Fem3 binding factor (PUF) family of RNA-binding proteins exhibit this type of post-transcriptional regulation of sets of transcripts specific for each of five Puf protein subtypes (García-Rodríguez et al., 2007; Olivas, 2000; Wang et al., 2018). Puf3 targets a module of about 220 transcripts that majorly includes nuclear-encoded mitochondrial proteins, which differ in their expression patterns during stress conditions influencing mitochondrial biogenesis (Gerber et al., 2004; Saint-Georges et al., 2008). While utilising carbon sources that demand active respiration, the repressor-like activity of Puf3 binding to the 3′-untranslated region (UTR) elements on the transcript decreases their expression by promoting degradation or preventing it (Miller et al., 2014; Olivas, 2000).

Various stress conditions, including osmotic, oxidative, nutritional deprivation, chemical, high temperature and so forth, were used to understand ESR in *Saccharomyces cerevisiae* (Causton et al., 2001; Gasch & Werner-Washburne, 2002; Morano et al., 2012). Studies in yeast strains from clinical and natural environments have linked genetic diversity to varying stress responses (Liti et al., 2009).

Mapping studies in segregating populations to determine causal loci for stress responses identified *MKT1*, a pleiotropic stress response gene mediating high-temperature growth (Sinha et al., 2008; Steinmetz et al., 2002), sporulation efficiency (Deutschbauer & Davis, 2005), chemical stress (Ehrenreich et al., 2010) and high ethanol concentration (Swinnen et al., 2012) in different yeast strains. Besides being causal for stress responses, *MKT1* is nonessential and alters mitochondrial stability, affecting stress response (Dimitrov et al., 2009; Wickner, 1987). At the molecular level, *MKT1* facilitates mating-type switching in yeast mother cells by selective post-transcriptional regulation of *HO* endonuclease during budding. Mkt1 interaction with Pbp1, a protein binding to poly-A binding protein, Pab1, supports the role of Mkt1 in the posttranscriptional regulation of transcripts selectively based on the consensus sequence on 3′-UTR of transcripts (Tadauchi et al., 2004). While S288c has *MKT1*^{89A}, nonsynonymous single-nucleotide polymorphism (SNP) changes *MKT1*^{A89G} substituting D30G in the polypeptide is conserved among various natural isolates (Liti et al., 2009). Allele replacement studies between SK1 and S288c have shown that *MKT1*(D30G) increases sporulation efficiency (Deutschbauer & Davis, 2005). Furthermore, genome-wide RNA expression analysis hypothesised that *MKT1*^{A89G} SNP variation could be causal in altering the transcript stability of Puf3 module genes under stress conditions (Lee et al., 2009; Sun et al., 2016). Similarly, quantitative trait loci (QTL) coding for *IRA2* was linked to regulating Puf4 activity and the causal polymorphisms were known to affect the transcripts encoding nucleolar ribosomal RNA-processing factors (Smith & Kruglyak, 2008).

While *MKT1* as a QTL influences the Puf3 targets, another locus, Pop7, positively regulates Puf3 activity (Fazlollahi et al., 2014).

Take-away

- *MKT1* alleles vary stress responses by posttranscriptional modulation of Puf3 targets.
- *PBP1* and *PUF3* influence the regulation of Puf3 target stability under stress.
- Nuclear-encoded mitochondrial Puf3 targets, *COX17*, *MRS1* and *RDL2*, contribute to the growth advantage of *MKT1*^{89G} allele in oxidative stress.

Additionally, overlapping targets between the Puf family proteins and the mechanism of network rewiring in the absence of Puf3 influence the expression of specific deletion phenotypes (Lapointe et al., 2017). In the current study, we link the allelic effects of *MKT1* with the stress-specific stability of Puf3 targets and elucidate the roles of *PBP1* and *PUF3* in this mechanism.

2 | MATERIALS AND METHODS

2.1 | Yeast strains and growth conditions

All the yeast strains used in the experiments are derivatives of the *Saccharomyces cerevisiae* S288c strain. The parental strains used were the 'S' strain (S288c-*MKT1*^{89A}) and the 'M' strain (S288c-*MKT1*^{89G}; Gupta et al., 2014). These strains were derived from the original strains obtained from Deutschbauer and Davis (2005). Briefly, the original strains were sequenced to confirm the allele replacements and then were backcrossed to the S288c strain for three generations to remove other mutations found in the strains. Gupta et al. (2015) used these backcrossed S and M strains for their whole-genome gene expression analysis.

Strains were grown in standard YPD (1% yeast extract, 2% peptone, 2% dextrose) medium at 30°C. Plasmid-based drug cassettes amplified using pFa6A (kanMX4), pAG25 (natMx4) and pAG32 (hphMX4) as templates (Goldstein & McCusker, 1999) were transformed to generate gene deletions in parental strains (Gietz et al., 1995). The stocks of H_2O_2 (TCI; Cat#H1222) and cycloheximide (CYC; Sigma; Cat#18079) were prepared in the water, while carbonyl cyanide *p*-(trifluoromethoxy) phenylhydrazone (FCCP; TCI; Cat#C3463) and 4-nitroquinoline 1-oxide (4NQO; Sigma; Cat#N8141) stocks were made in dimethylsulphoxide. These chemicals were added to YPD and used for stress conditions. The final concentrations used for each assay are given below.

2.2 | Spot dilution assay

A saturated culture from a single colony was obtained for 5 mL of YPD after overnight incubation at 30°C. A dilution of 1:100 of saturated culture was used for cell counting using a haemocytometer.

A serial dilution series ranging from 10^8 to 10^3 cells/mL was made for each strain. Five microliters of each dilution in the series were used to spot on YPD (control) and plates containing YPD along with stress agents (8% ethanol, 0.002% H_2O_2, 0.4 μg/mL 4NQO, 0.25 μg/mL CYC and 6 μg/mL FCCP). The plates were incubated for 4 days at 30°C, following which the growth was recorded. Stress resistance was measured by comparing the number of spots with growth. All strains used for this study were diploid except for growth kinetics experiments, which were haploid. All the strains used in this study are given in Table S1 and the primers in Table S2.

2.3 | Growth kinetics

Turbid culture of strains in YPD was obtained in 96-well cell culture plates after 24 h incubation at 30°C with 250 rpm. Experiments were performed in 96-well cell culture plates, with each sample represented in triplicates of 200 μL/well. Each strain was grown in YPD as a control for assays indicated with different chemicals CYC (0.1 μg/mL), 4NQO (0.3 μg/mL), H_2O_2 (0.01%) and FCCP (1 μg/mL). The plate was incubated for 42 h at 30°C at 355 cpm (orbital), and OD600 was recorded every 30 min using a BioTek EPOCH2 microplate reader. The growth curves were used to compute the growth rate and corresponding relative fitness. The relative fitness was defined as a ratio of the growth rate under the test condition to the growth rate in control (YPD) for the same strain.

2.4 | Fluorescence measurements

M and S strains with green fluorescent protein (GFP)-tagged *MKT1* were used for fluorescence studies to compare the levels of native protein expression. The strains with C-terminal GFP tagging were generated using pYM25 and selected with a hygromycin marker (Janke et al., 2004). The overnight culture was used to inoculate fresh media and was grown till 1 OD absorbance at 600 nm. The culture was spun down and washed three times with phosphate-buffered saline (PBS) (pH 7.4). The pellet was resuspended in 2 mL fresh PBS, and the suspension was diluted to 1 OD. Three hundred microlitres of cell suspension was pipetted in each well in a black opaque 96-well plate as well as 96-well transparent tissue culture plate to measure fluorescence at Em/Ex 485/510 nm and absorbance at 600 nm, respectively, using BioTek multimode plate reader (Synergy H1). PBS was used as blank, and a strain without GFP was used as a negative control. The fluorescence intensity of each well is divided by the corresponding absorbance to get normalised fluorescence intensity, which was represented as the average of biological replicates.

2.5 | RNA extractions

To study the temporal degradation kinetics of a candidate messenger RNA (mRNA), 1,10-phenanthroline (Sigma; Cat#131377) was used as a transcription inhibitor at a concentration of 200 μg/mL in YPD and stress conditions. The overnight culture was measured at OD600 and inoculated to grow from 0.2 to 0.8 OD in YPD (control). For stress conditions, cultures were grown from 0.8 to 1.0 OD after adding stress-inducing agents to the required concentrations of CYC (3 μg/mL), 4NQO (2 μg/mL), H_2O_2 (0.15%) and FCCP (20 μg/mL). Later, 1,10-phenanthroline was added to control and stress cultures. Samples were collected every 15 min after administration of the drug, for which 10 mL of culture corresponding to a particular time point was spun down at 8000 rpm for 30 s, and the pellet was snap-frozen using liquid nitrogen.

Frozen cell pellets transferred to 1.5 mL tubes were added with 50 μL of phenol–chloroform–isoamyl alcohol (25:24:1 ratio; PCI) (Sigma; Cat#71617), 50 μL of Lysis buffer (50 mM Tris pH 7–7.4, 130 mM NaCl, 5 mM EDTA, 5% sodium dodecyl sulphate) and glass beads (approximately 2/3 of the pellet volume) was added to the tube. The tubes were then vortexed at maximum speed for 20 min at 4°C, followed by centrifugation at 13,000 rpm for 15 min at 4°C. The aqueous layer was transferred to precooled 0.5 mL tubes, and an equal volume of PCI was added. After vigorous mixing, the mix was centrifuged at 13,000 rpm for 10 min at 4°C. This step was repeated. The aqueous layer was extracted, and an equal volume of chloroform–isoamyl alcohol (24:1 ratio) was added. After vigorous mixing, the mix was centrifuged at 13,000 rpm for 10 min at 4°C. The step was repeated. The aqueous layer was removed and transferred to precooled Eppendorf tubes containing 1/20th volume of 3 M sodium acetate and two volumes of absolute ethanol. Total RNA was precipitated by inverting tubes and incubating them at −20°C for 30 min, followed by centrifugation at 13,000 rpm for 15 min. The pellet was washed using 200 μL of 80% ethanol and centrifuged for 2 min without disrupting the pellet. The supernatant was discarded, and the pellet was air-dried on ice for 30 min.

The pellet was resuspended in a buffer containing TURBO DNase (Invitrogen; Cat#8167) following the manufacturer's instructions to remove genomic DNA contamination. The concentration of RNA in the resulting solution was measured using Nanodrop; a ratio of approximately 2.0 for 260/280 and 260/230 was considered suitable for further studies. One microgram of the sample was run on 2% agarose gel with ethidium bromide used to assess the integrity of the RNA sample.

2.6 | Quantitative gene expression studies

According to the manufacturer's instructions, 3.125 μg of RNA was used for complementary DNA (cDNA) synthesis using random hexamers (Invitrogen; Cat#N8080127) for priming and enzyme Superscript III (Invitrogen; Cat#18080093). From which 25 ng of cDNA was used per quantitative PCR (qPCR) reaction of 10 μL using KAPA SYBR FAST (Sigma; Cat#KK4618) master mix and primers. The reaction was carried out with Analytikjena qTOWER3 in a two-step cycle of denaturation at 95°C and annealing and elongation at 60°C for 35 cycles. The C_t values from the experiments were used to

calculate the respective ΔC_t (Costa et al., 2013) and $\Delta\Delta C_t$ values, which were used for further analysis. ΔC_t was calculated as $C_{t(\text{gene of interest})} - C_{t(\text{endogenous control gene})}$, while $\Delta\Delta C_t$ was calculated as $\Delta C_{t(\text{treated sample})} - \Delta C_{t(\text{untreated control sample})}$. $\Delta\Delta C_t$ were obtained using ΔC_t of the initial time point as a control sample for all the time points in that series after adding 1,10-phenanthroline. ΔC_t values of tested genes were used in expression and linear regression analyses between *MKT1* allelic backgrounds. Temporal $\Delta\Delta C_t$ values were used in differential stability analysis using Chow's test (Chow, 1960).

3 | RESULTS

3.1 | *MKT1* alleles contribute differentially to growth phenotype during stress

The phenotyping using serial dilutions (Figure 1a) showed that while in control conditions (YPD), there was no difference between the M and S strains, under stress growth conditions—ethanol, H_2O_2, FCCP, 4NQO and CYC, the M strain grew better than the S. A series of concentrations ranging from 2% to 10% ethanol, 0.005%–0.04% H_2O_2, 0.2–0.8 μg/mL CYC and 4NQO and 0.1–10 μg/mL FCCP were tested for differences in growth phenotype. These phenotyping results were confirmed using haploids with growth kinetic assays where no difference was observed between the M and S strains in YPD; in stress, the M had better growth rate and relative fitness than the S strain (Figure 1b,c). In both the spot dilution and growth kinetics assays, the concentration of stress-inducing agents was optimised to provide observable phenotypic differences between M and S backgrounds. While spot dilution assays in media containing ethanol showed a prominent growth difference between M and S strains, it was omitted from further experimentation due to its volatility and prolonged doubling time induced by the lack of glucose.

The phenotypic assays of the M and S strains showed that *MKT1* was dispensable in a stress-free environment, and the levels of *MKT1* in both backgrounds showed no difference (Supporting Information S1: Figures S1 and S2). However, the M strain was advantageous for growth rate and relative fitness in stress conditions over the S strain. While spot dilution experiments inferred a better phenotype of the M strain in H_2O_2 and FCCP, the relative fitness of both allelic strains was similar due to the lower chemical concentrations used for liquid cultures.

3.2 | *PBP1* and *PUF3* affect the magnitude and direction of *MKT1*^{89G}-mediated growth advantage during stress

To understand the role of *PBP1* and *PUF3* in *MKT1*-mediated stress responses, *pbp1Δ*, *puf3Δ* and *pbp1Δpuf3Δ* deletions were generated in M and S backgrounds. Growth kinetics assays in YPD showed that deleting *pbp1* or *puf3* or both had no effect in M and S backgrounds (Supporting Information S1: Figure S3). Not surprisingly, the M-*pbp1Δ* strain had better relative fitness than S-*pbp1Δ* in CYC and 4NQO. However, the S-*pbp1Δ* strain showed better relative fitness than M-*pbp1Δ* in H_2O_2 and FCCP (Figure 2a).

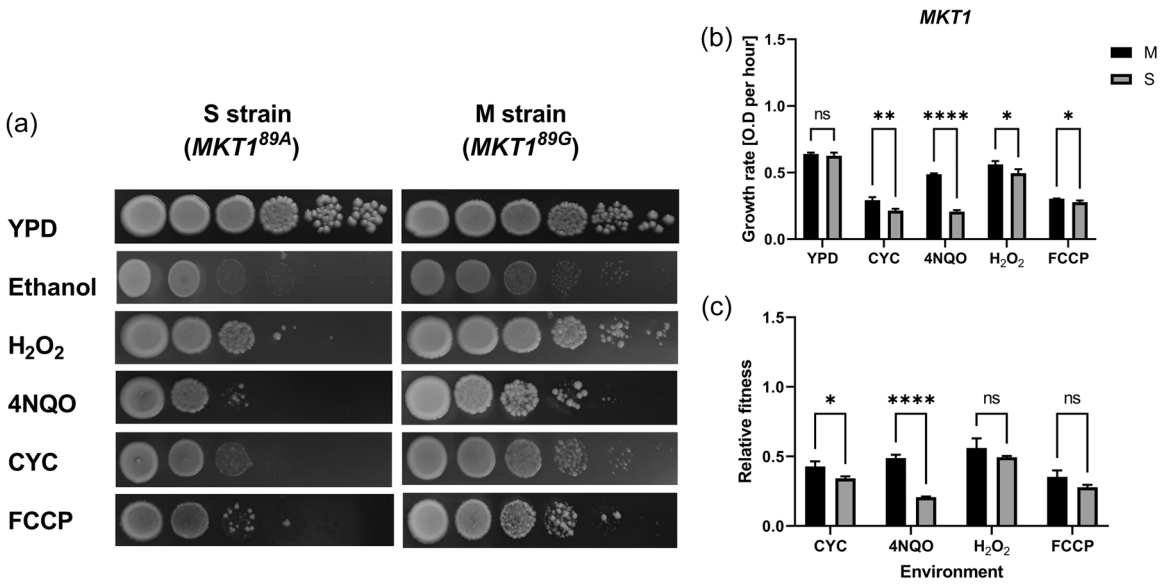

FIGURE 1 Analysis of *MKT1* allelic variants for pleiotropic stress resistance. (a) Ten-fold serial dilution ranging from 10^8 to 10^3 cells/mL of S and M strains were spotted on YPD (1% yeast extract, 2% peptone, 2% dextrose), 8% ethanol, 0.02% H_2O_2, 0.4 μg/mL 4-nitroquinoline 1-oxide (4NQO), 0.25 μg/mL cycloheximide (CYC) and 6 μg/mL carbonyl cyanide *p*-(trifluoromethoxy) phenylhydrazone (FCCP). Comparison of (b) growth rates and (c) relative fitness between M and S strains across YPD, 0.1 μg/mL CYC, 0.3 μg/mL 4NQO, 0.01% H_2O_2 and 1 μg/mL FCCP. The experiments were performed in triplicates, and the error bars represent SD. *p* Values were calculated using a *t*-test, and significance was indicated as ns, nonsignificant, $^*p < 0.05$, **0.001 and ****<0.00001 on the top of each comparison.

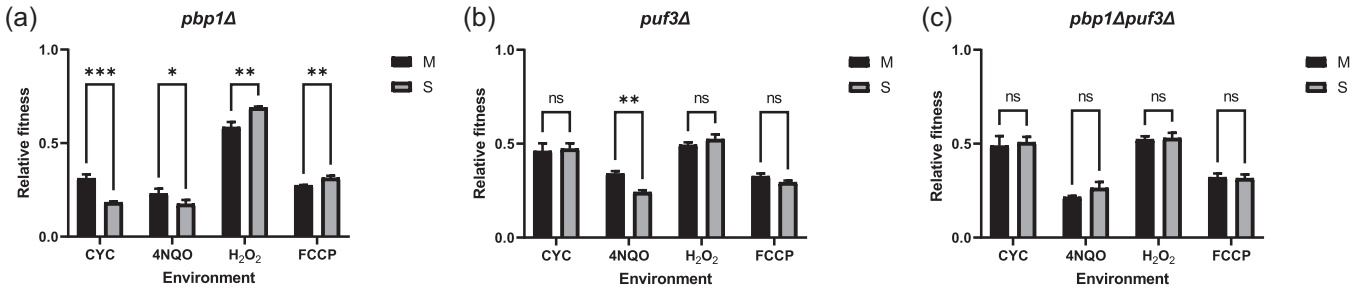

FIGURE 2 Role of *PBP1* and *PUF3* in *MKT1*-mediated stress responses. Relative fitness between M and S backgrounds with (a) *pbp1Δ*, (b) *puf3Δ* and (c) *pbp1Δpuf3Δ* deletions across YPD (1% yeast extract, 2% peptone, 2% dextrose), 0.1 μg/mL cycloheximide (CYC), 0.3 μg/mL 4-nitroquinoline 1-oxide (4NQO), 0.01% H_2O_2 and 1 μg/mL carbonyl cyanide *p*-(trifluoromethoxy) phenylhydrazone (FCCP). The experiments were performed in triplicates, and the error bars represent SD. *p* Values were calculated using a *t*-test, and significance was indicated as ns, nonsignificant, $^*p < 0.05$, $^{**}<0.001$ and $^{***}<0.0001$ on the top of each comparison.

No difference in relative growth was observed between M-*puf3*Δ and S-*puf3*Δ strains in YPD, CYC, H_2O_2 and FCCP (Supporting Information S1: Figure S4). However, M-*puf3Δ* had higher relative fitness than S-*puf3*Δ in 4NQO (Figure 2b and Supporting Information S1: Figure S2B).

As expected, double deletion strains of *pbp1Δpuf3Δ* in M or S backgrounds showed no growth difference in all the environments tested (Figure 2c). Thus, the double deletion of *pbp1* and *puf3* affected M and S backgrounds similarly, masking any individual allelic effects observed in the stress environments.

Analysing the *MKT1* allele and gene interactions across the environments showed that *PBP1* affected growth in CYC and H_2O_2, while *PBP1* with *PUF3* contributed to growth in 4NQO (Supporting Information S1: Figure S4). This indicated that *MKT1*-mediated stress responses could employ both *PUF3* and *PBP1* in an environment-dependent manner.

3.3 | *MKT1* alleles control the expression levels of Puf3 targets using posttranscriptional machinery

We wanted to determine the expression levels of Puf3-target and Puf3-independent genes in each environment and background (M and S, Tables 1 and S3). These genes were chosen to encompass diverse functional ranges like transfer RNA (tRNA) synthesis, splicing, translation and ribosomal proteins to find their involvement in different stress conditions. Therefore, we analysed the expression differences using ΔC_t values of these genes at the initial time point between M and S backgrounds across multiple environments (Figure 3a). The initial differences in the expression of tested genes between M and S backgrounds across the environments are given in Table S4.

It was observed that some of the Puf3 targets, such as *MEF1*, *MRPL6*, *PET123* and *RSM24*, showed higher expression in M compared to the S strain across three or more environmental conditions. In YPD, even though *MKT1* alleles did not show any growth differences, a few of the Puf3-target genes *MSF1*, *RSM24*, *NAM2*, *MRS1* and *MEF1* were already differentially expressed at the initial time point. However, in CYC, 4NQO, H_2O_2 and FCCP, while there was a growth difference between M and S strains, some of the Puf3-target genes were differentially expressed between the two strains, with M allele strains showing higher expression (Figure 3a). Furthermore, all genes with nonmitochondrial function had no expression difference between M and S strains in YPD (Table 2). The temporal ΔC_t plots of each gene for all the conditions tested were given in Supporting Information S1: Figures S5–S9.

In CYC and H_2O_2, where growth differences were observed between *MKT1* alleles, more genes were differentially expressed compared to other stress conditions. From the tested environments, including YPD, the expression levels in all the genes that showed differential expression were higher in the M compared to the S strain. This indicated that the M allele contributed to the differential expression by overexpressing some Puf3 targets in all the environments.

Interestingly, we observed that a few of the Puf3-target mitochondrial ribosome protein genes, *MRPL6*, *PET123* and *RSM24*, showed differential expression and stability in stress environments (Figure 3a,b). Several reports (Genuth & Barna, 2018) indicate that ribosomal protein genes differentially translate a set of transcripts in a stress-dependent manner. Therefore, we did not analyse these genes further to avoid this ribosomal heterogeneity as a confounding factor.

It has been previously shown that *MKT1* activity depends on Pbp1 (Tadauchi et al., 2004). Furthermore, Lee et al. (2009) showed that *MKT1* played a role in the RNA stability of Puf3-dependent transcripts. To test if the differences described above depended on Puf3 and Pbp1, we deleted these genes in M and S backgrounds and measured expression levels at the initial time for a subset of Puf3-target genes (Figure 3b). This set of genes was selected based on the variable expression differences observed in wild type in different growth conditions (Table 2). To obtain an unbiased estimate of the phenomenon due to the deletion of Pbp1 and Puf3, the established Puf3 target *COX17* (Olivas, 2000) was omitted from this list of tested genes. As H_2O_2 showed the maximum number of differentially expressed genes relative to other stress conditions, we chose to study the roles of *PBP1* and

TABLE 1 List of genes analysed using RT-qPCR studies.

Puf3 affinity	Function	Gene
Puf3 targets	Mitochondrial	*ARG2, COX17, MEF1, MRF1, MRPL6, MRS1, MSD1, MSF1, MSS2, NAM2, PET123, RDL2, RSM24, SUV3, TIM44*
	Nonmitochondrial	*CCC2, CTM1, HIR1, HOT1, IVY1, KEL2, MSB3, UBP16, YNG2*
Non-Puf3 targets	Mitochondrial	*ECM10, RNR3*

Note: Candidate Puf3 targets were selected from Gerber et al. (2004), and non-Puf3 targets were selected from SGD (https://www.yeastgenome.org/). Abbreviation: RT-qPCR, real-time quantitative PCR.

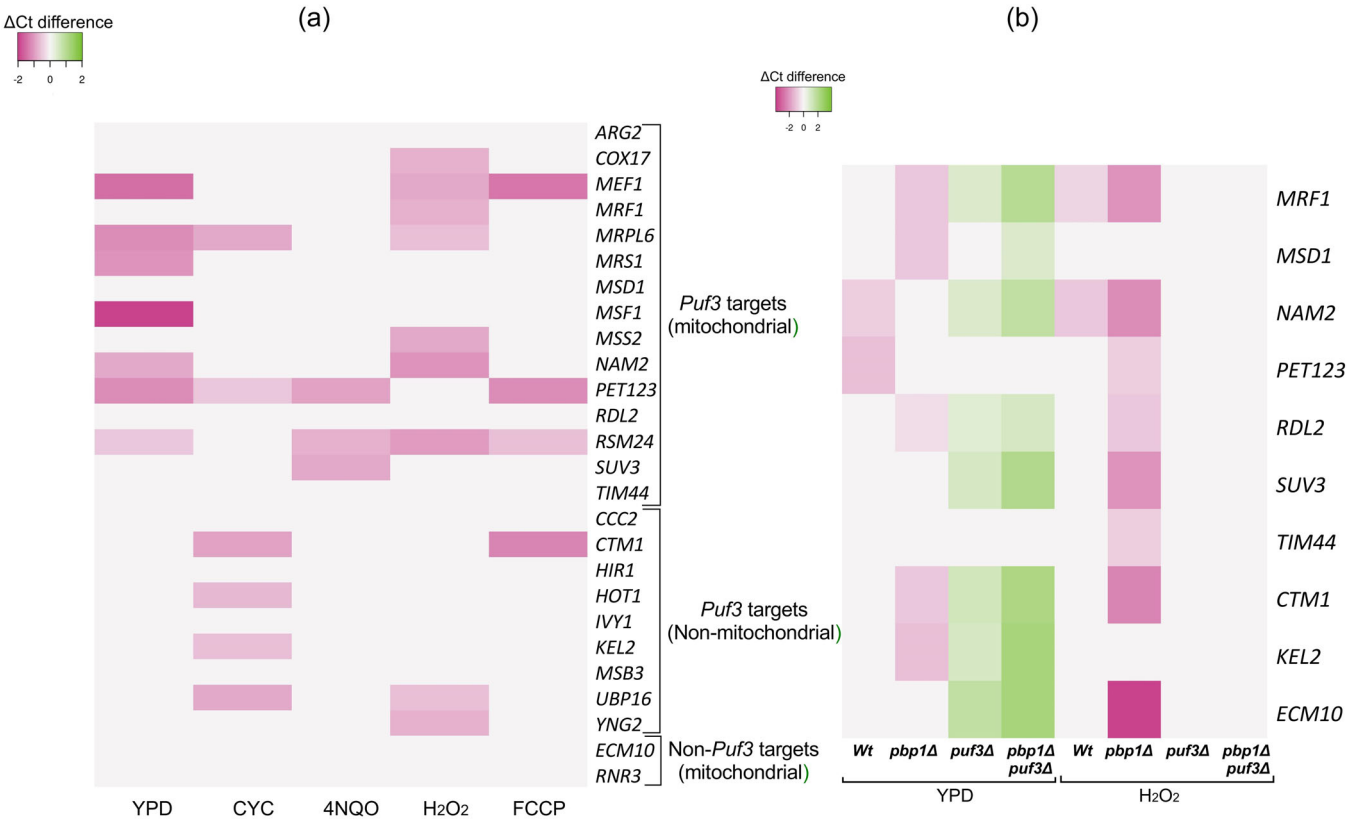

FIGURE 3 Differential expression (ΔC_t) of Puf3 targets between M and S backgrounds at initial time point (a) wild type across multiple environments, (b) *pbp1Δ*, *puf3Δ* and *pbp1Δpuf3Δ* deletions across YPD and H_2O_2. Cells were grown in YPD (control), CYC (3 μg/mL), 4NQO (2 μg/mL), H_2O_2 (0.15%) and FCCP (20 μg/mL). The experiments were performed in triplicates, and the significant differences ($p < 0.05$) in ΔC_t between M and S backgrounds were reported. 4NQO, 4-nitroquinoline 1-oxide; CYC, cycloheximide; FCCP, carbonyl cyanide *p*-(trifluoromethoxy) phenylhydrazone; YPD, 1% yeast extract, 2% peptone, 2% dextrose.

PUF3 in the H_2O_2 environment to compare against YPD control. In the *pbp1Δ* background, both in YPD and H_2O_2, for all the differentially expressed genes, the expression in M-*pbp1*Δ was higher than S-*pbp1*Δ. However, in the *puf3*Δ background, differentially expressed genes were observed in YPD alone, but interestingly, the expression of these genes was higher in the S-*puf3*Δ than in the M-*puf3*Δ strain. This is similar to the previous observations where Puf3 facilitated degradation in YPD but not under stress conditions (Miller et al., 2014). Comparison of the results between single deletions, *pbp1Δ* and *puf3*Δ, and double deletion *pbp1Δpuf3Δ* backgrounds showed that the differential expression of the genes was Puf3-dependent.

To understand if this differential expression of Puf3-target genes affected their transcript stability, the transcript levels were measured at regular intervals (15 min each till 60 min endpoint) after adding 1,10-phenanthroline. The ΔC_t slopes of temporal samples of each Puf3-target gene were calculated using linear regression in the M and S strains and were compared in different environments. This comparison was made to determine if there was a change in the stability of the transcripts of Puf3-target genes for both wild-type M and S strains in YPD and H_2O_2, Puf3-target gene slopes were highly correlated ($R^2 = 0.83$, $p = 0.005$) and ($R^2 = 0.78$, $p = 0.013$, respectively). This observation suggested that in wild-type strains, all the Puf3-target gene transcripts behaved similarly for both

TABLE 2 List of genes showing differential expression of transcripts between M and S strains under each growth condition.

Environment	Puf3 targets showing differential expression
YPD	*MEF1, MRPL6, MRS1, MSF1, NAM2, PET123, RSM24*
CYC	*MRPL6, PET123, CTM1, HOT1, KEL2, UBP16*
4NQO	*PET123, RSM24, SUV3*
H_2O_2	*COX17, MEF1, MRF1, MRPL6, MSS2, NAM2, RSM24, UBP16, YNG2*
FCCP	*MEF1, PET123, RSM24, CTM1*

Abbreviations: 4NQO, 4-nitroquinoline 1-oxide; CYC, cycloheximide; FCCP, carbonyl cyanide *p*-(trifluoromethoxy) phenylhydrazone; YPD, 1% yeast extract, 2% peptone, 2% dextrose.

environments, that is, stabilised or degraded. For the *pbp1*Δ strain, in M and S backgrounds, Puf3-target gene slopes were only correlated in YPD ($R^2 = 0.66$, $p = 0.03$) and not H_2O_2 ($R^2 = 0.18$, $p = 0.6$). However, for the *puf3*Δ strain, in M and S backgrounds, only in H_2O_2, Puf3-target gene slopes were correlated ($R^2 = 0.89$, $p = 0.0005$), whereas in YPD ($R^2 = 0.05$, $p = 0.87$) no correlation was observed. These results indicated that in H_2O_2, Puf3-target gene transcripts were under Pbp1 regulation. The temporal ΔC_t plots of each of the genes analysed under the deletion backgrounds of *pbp1*Δ, *puf3*Δ and *pbp1*Δ*puf3*Δ for all the conditions tested were given in Supporting Information: Figures S10–S12.

3.4 | *PBP1* and *PUF3* interact differentially with *MKT1*^{89G} allele to stabilise Puf3 targets

Therefore, to check if these accessory proteins differentially altered transcript stability in an *MKT1* allele-specific manner in H_2O_2, we studied *pbp1*Δ, *puf3*Δ *and pbp1*Δ*puf3*Δ in the M and S backgrounds and compared transcript degradation patterns with wild type using temporal RT-qPCR assay (Figure 4). Using the initial point sample as a control for the temporal qPCR data $\Delta\Delta C_t$ values were computed, and their median was used as a metric to measure the stability of Puf3 targets after the transcriptional stop. In the wild type for YPD ($p = 0.99$) and H_2O_2 ($p = 0.23$), there was no significant difference between the median $\Delta\Delta C_t$ of the M and S strains. However, when the median $\Delta\Delta C_t$ values of the M strain were compared between YPD and H_2O_2, it was observed that the Puf3 targets were preferentially stabilised in H_2O_2 ($p < 10^{-3}$; Figure 4a). This stabilisation of Puf3 targets was also observed in the S strain between YPD and H_2O_2 ($p < 10^{-3}$; Figure 4a). This indicated that the degradation rates of Puf3 targets in M and S strains were similar in YPD and H_2O_2. However, in YPD, between M-*pbp1*Δ and S-*pbp1*Δ strains, there was a significant difference in the degradation rates for most Puf3 gene transcripts ($p < 10^{-3}$; Figure 4b). The lower the median $\Delta\Delta C_t$ value, the more stabilised the Puf3 transcripts. In H_2O_2, similarly, S-*pbp1*Δ had more stabilised transcripts than the M-*pbp1*Δ ($p < 10^{-3}$; Figure 4b). However, when a comparison was made between M-*pbp1*Δ across YPD and H_2O_2, there was a significant difference in stability, with the transcripts in YPD being more stable than in H_2O_2 ($p = 0.004$; Figure 4b). This was not the case for transcripts across the two environments in S-*pbp1*Δ ($p = 0.24$; Figure 4b). This observation indicated that the role of Pbp1 in transcript stabilisation was more prominent in the M than in the S strain. In the *puf3*Δ deletion background, the observations were similar to the *pbp1*Δ background, with significant differences between the M and S backgrounds in YPD ($p = 0.03$) and H_2O_2 ($p < 10^{-3}$). Puf3 is a known regulator of Puf3 targets in nonstress conditions like YPD (Olivas, 2000). Therefore, we observed that in the absence of *puf3*Δ in the M background, the Puf3 transcripts were stabilised more than what was observed in the wild-type M background (Figure 4a,c). Finally, in the *pbp1*Δ*puf3*Δ deletion strains in the M and S backgrounds, the patterns of the Puf3 transcript stability remained similar to what was observed in the *puf3*Δ and *pbp1*Δ backgrounds. However, in this case, the absence of *pbp1*Δ*puf3*Δ in both backgrounds stabilised the Puf3 transcripts more than observed in the wild-type backgrounds (Figure 4a,d). These results indicated in YPD that Pbp1 had a stabilising effect while Puf3 had a destabilising effect on Puf3 target transcripts. However, the roles of Pbp1 and Puf3 were concordant in H_2O_2. Therefore, there was an environment-dependent stabilisation of Puf3-target genes in the M background, indicating that Pbp1 and *MKT1* alleles regulate mRNA levels posttranscriptionally.

We wanted to test whether *MKT1* alleles differentially affect the stability of Puf3 targets across the environments. Temporal mRNA samples were analysed using transcript-specific RT-qPCR assay to monitor transcript decay rates for each transcript in the M and S backgrounds and across environments. The resulting temporal $\Delta\Delta C_t$ values of each transcript in both M and S backgrounds were compared, and Chows' test was used to determine significance. In YPD, all the genes except *HIR1*, *MSB3* and *MSD1* showed nonsignificant differences in the stability between the *MKT1* alleles. However, some Puf3-target gene transcripts showed significant variation in their stability rates between the *MKT1* alleles (Table 3). For example, in CYC, *COX17*, *MRS1*, *RDL2* and 4NQO, *PET123*, *RDL2*, and *YNG2* significantly varied in their stability rates between the two *MKT1* alleles. The differentially stabilised transcripts belonged to mitochondrial and non-mitochondrial Puf3-target genes.

3.5 | *COX17*, *MRS1* and *RDL2* are essential for the M strain to maintain growth advantage in stress environments

To understand the role of differentially expressed Puf3 targets in the pleiotropic stress response of MKT1 alleles, we curated a subset of Puf3 targets to study their roles by deleting them in both M and S backgrounds. Puf3 targets—*COX17*, *IVY1*, *MRF1*, *MRS1*, *MSD1* and *RDL2*—were selected based on their differential expression and varying stability between the *MKT1* alleles observed in qPCR assays. *COX17* and *MRS1* were observed to be both differentially expressed and differentially stabilised. *MRF1* represents differential expression

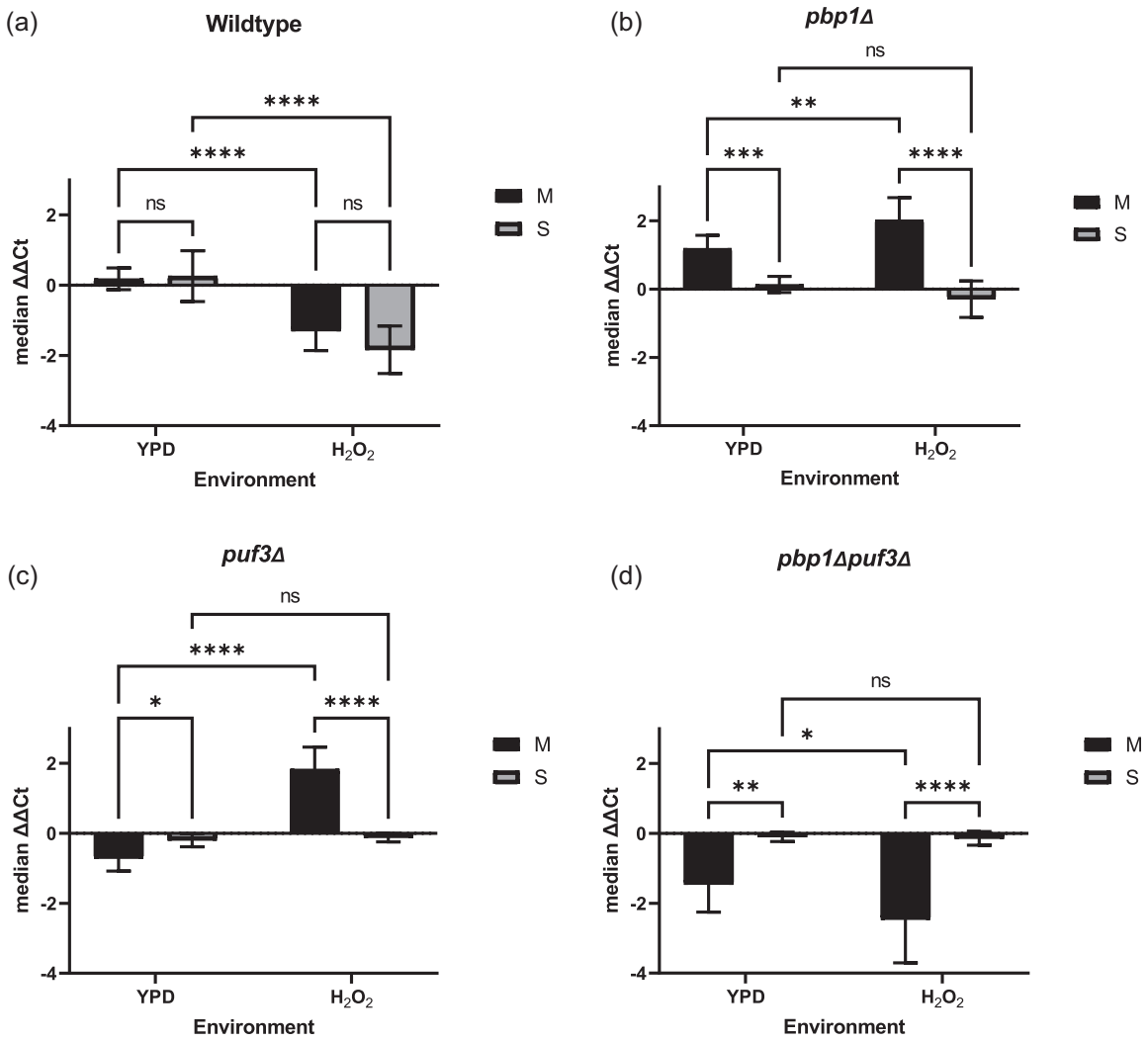

FIGURE 4 Analysis of temporal median $\Delta\Delta C_t$ values among Puf3 targets between M and S backgrounds in (a) wild type, (b) *pbp1Δ*, (c) *puf3Δ* and (d) *pbp1Δpuf3Δ* deletions across YPD and H_2O_2 (0.15%). The experiments were performed in triplicates, and the error bars represent SD. *p* Values were calculated using analysis of variance, and significance was indicated as ns, nonsignificant, *$p < 0.05$, **0.001, ***0.0001 and ****0.00001 on the top of each comparison. YPD, 1% yeast extract, 2% peptone, 2% dextrose.

TABLE 3 List of genes showing differential degradation of transcripts between M and S strains under each growth condition.

	Genes showing differential degradation	
Environment	**Puf3 targets**	**Non-Puf3 targets**
YPD	*HIR1, MSB3, MSD1*	
CYC	*COX17, MRS1, RDL2,*	*RNR3*
4NQO	*PET123, RDL2, YNG2*	
H_2O_2	*RSM24*	
FCCP	*PET123, SUV3*	*RNR3*

Abbreviations: 4NQO, 4-nitroquinoline 1-oxide; CYC, cycloheximide; FCCP, carbonyl cyanide *p*-(trifluoromethoxy) phenylhydrazone; YPD, 1% yeast extract, 2% peptone, 2% dextrose.

alone. Similarly, *MSD1* and *RDL2* have shown differential degradation alone. *IVY1* was selected as a nonmitochondrial gene with no differential expression between *MKT1* alleles. *COX17* acts as a copper metallochaperon in mitochondria (Heaton et al., 2000). Phospholipid-binding protein *IVY1* regulates vacuole fission (Lazar et al., 2002). *MRF1* is a mitochondrial translation release factor (Pel et al., 1992). RNA-binding protein *MRS1* controls RNA processing via splicing Group I introns in mitochondria (Kreike et al., 1986). *MSD1* is a mitochondrial aspartyl-tRNA synthetase (Gampel & Tzagoloff, 1989). *RDL2* is a mitochondrial thiosulfate sulfurtransferase (Foster et al., 2009).

We grew these gene deletion strains in CYC (0.1 μg/mL), 4NQO (0.3 μg/mL) and H_2O_2 (0.01%) and compared their growth between M and S across wild-type, *pbp1Δ*, *puf3Δ* and *pbp1Δpuf3Δ*

backgrounds for each environment. The concentrations of these chemicals in these liquid culture assays, even within the range tested, were lower than those used in the spot dilution assays. Lower concentration was used in liquid culture to allow these wild-type and deletion strains to grow in liquid media. The phenotype difference between M and S in wild type was used to compare the effect of specific gene deletion in the respective environment.

In the wild type, as shown previously, the M strain grew better than the S in CYC (Figure 5a). When *PBP1* was deleted, the M strain was still better than the S. However, the fitness advantage for the M strain over the S was lost when either *puf3*Δ or *pbp1*Δ*puf3*Δ were deleted. This indicated that in CYC, the growth advantage of the M allele was *PUF3*-dependent, and *PUF3* was epistatic over *PBP1*. In 4NQO, in the wild type, the fitness advantage of the M strain over the S was independent of *PBP1* and *PUF3*, but when both these genes were deleted, no difference was observed (Figure 5e). This observation showed that in 4NQO, both *PBP1* and *PUF3* had an additive effect on growth. In the wild type, no significant growth differences were observed in H_2O_2 for any strain.

In the *cox17*Δ background in both the M and S strains, the roles of *PBP1* and *PUF3* were altered. Compared to the wild type, *PBP1* and *PUF3* were required in CYC for the growth advantage of the M allele (Figure 5b). Therefore, *PUF3* was no longer epistatic over *PBP1* in this background. Similarly, in 4NQO, compared to the wild type, no growth difference was observed in either *pbp1*Δ or *puf3*Δ (Figure 5f). This indicated that *COX17* was required for *PBP1* and *PUF3*-dependent growth advantage of the M strain in all three environments.

In the *mrs1*Δ background, similar to the wild type, in CYC and 4NQO, the deletion of *pbp1*Δ resulted in a growth advantage of the M strain over the S (Figure 5c,g). However, in contrast to the wild type, the deletion of *puf3*Δ resulted in a reversal of the growth advantage, with the S strains growing better than the M. This reversed phenotype was also observed in the *pbp1*Δ*puf3*Δ double deletion background. This indicated that first, the growth advantage of the M allele was *PUF3*-dependent, and second, in the *mrs1*Δ background, *PUF3* was required for the activity of the M allele.

In the *rdl2*Δ background, in CYC, the growth advantage of the M strain was dependent on *PBP1*, with *PBP1* being epistatic over *PUF3* as the double deletion *pbp1*Δ*puf3*Δ was similar to *pbp1*Δ alone (Figure 5d). In 4NQO, again, the effect of *RDL2* was *PBP1*-dependent (Figure 5h). Interestingly, in 4NQO, deletion *pbp1*Δ resulted in the S strain having better growth than the M. Compared to the *MRS1* result, where better growth of the S strain was found to be dependent on *PUF3*, here in *RDL2*, it was dependent on *PBP1*. This indicated that in the same environment, the effects and roles of *PBP1* and *PUF3* are genetic background dependent.

In the H_2O_2 environment, there was no difference between the M and S strains in the wild type, even when *pbp1*Δ and *puf3*Δ were deleted singly or in combination (Figure 6a). Interestingly, in *cox17*Δ, *mrs1*Δ and *rdl2*Δ backgrounds, the M strain was better than the S (Figure 6b–d). But, when in these backgrounds, either *pbp1*Δ or *puf3*Δ

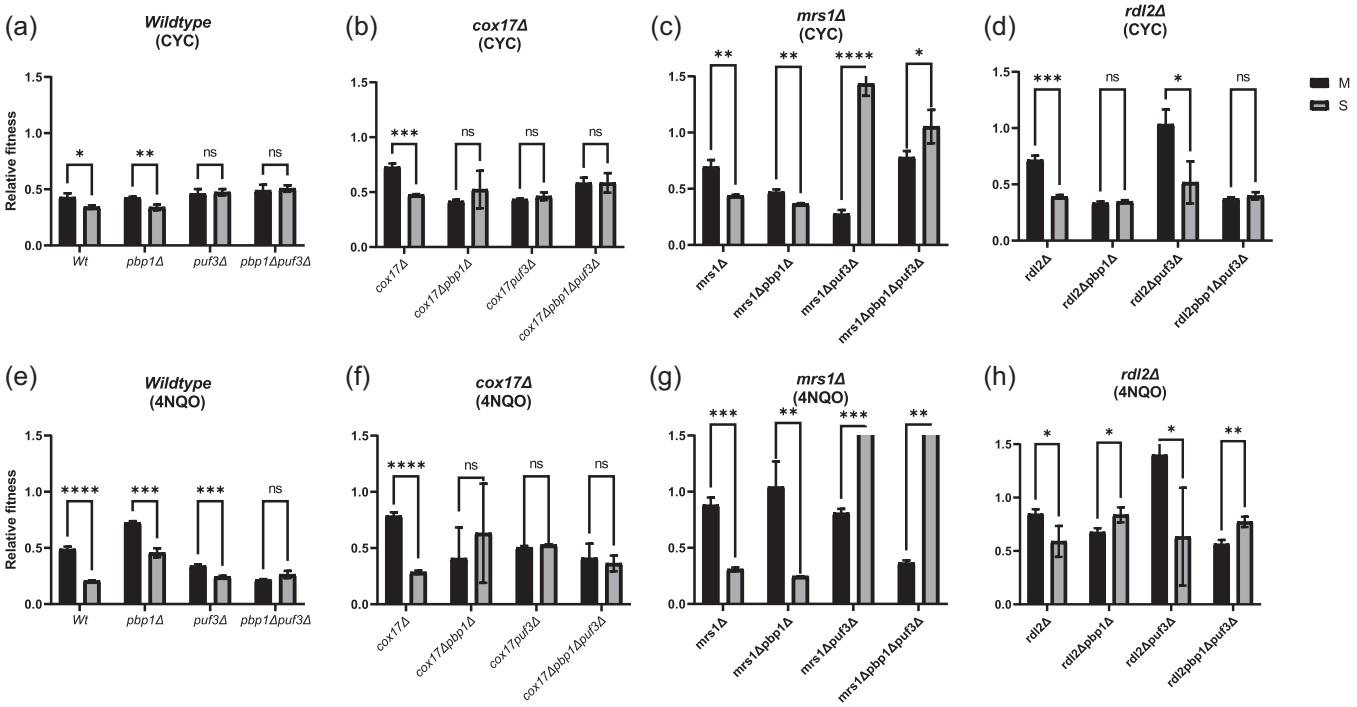

FIGURE 5 Effect of *COX17*, *MRS1* and *RDL2* on *MKT1* allelic response in cycloheximide (CYC) and 4-nitroquinoline 1-oxide (4NQO). Comparison of relative fitness between *MKT1* alleles in wild-type, *cox17Δ*, *mrs1Δ* and *rdl2Δ* backgrounds and the effect of wild type, *pbp1Δ*, *puf3Δ* and *pbp1Δpuf3Δ* for each deletion in (a–d) 0.1 μg/mL CYC and (e–h) 0.3 μg/mL 4NQO. The experiments were performed in triplicates, and the error bars represent SD. *p* Values were calculated using a *t*-test, and significance was indicated as ns, nonsignificant, **p* < 0.05, **0.001, ***0.0001 and ****0.00001 on the top of each comparison.

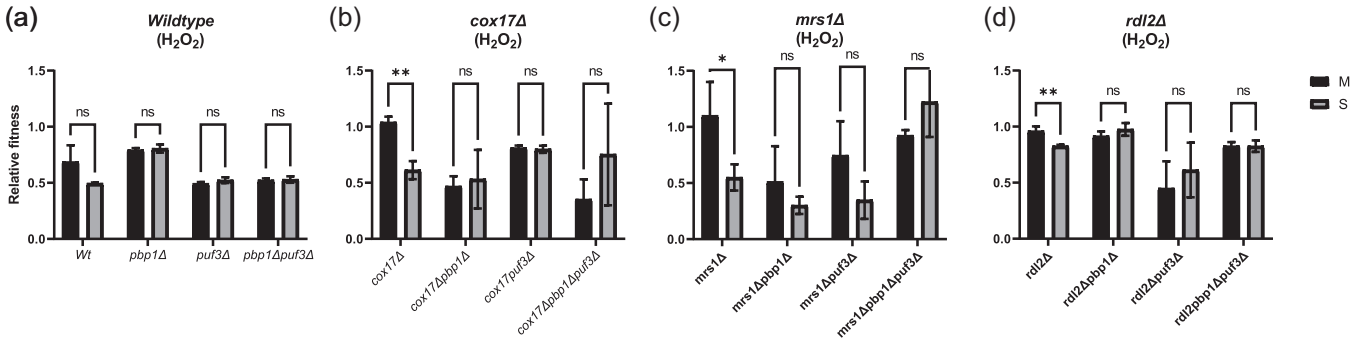

FIGURE 6 Effect of *COX17*, *MRS1* and *RDL2* on *MKT1* allelic response in H_2O_2. Comparison of relative fitness between *MKT1* alleles in wild type, *cox17Δ*, *mrs1Δ* and *rdl2Δ* backgrounds and the effect of wild type, *pbp1Δ*, *puf3Δ* and *pbp1Δpuf3Δ* for each deletion in (a–d) 0.01% H_2O_2. The experiments were performed in triplicates, and the error bars represent SD. *p* Values were calculated using a *t*-test, and significance was indicated as ns, nonsignificant, *$p < 0.05$ and **0.001 on the top of each comparison.

or *pbp1Δpuf3Δ* were deleted, the growth advantage of the M strain was lost. This indicated that the *Puf3*-dependent nuclear-encoded mitochondrial genes were required for better growth of the S strain, meaning that the nonfunctional allele of *MKT1* needed these genes for proper growth. This conclusion was further supported by deletion phenotypes of *msd1Δ* and *mrf1Δ*, which showed a similar phenotype pattern as *cox17Δ* (Supporting Information S1: Figure S13F,I). For a nonmitochondrial gene, like *IVY1*, the deletion of *ivyΔ* was the same as wild-type phenotype, indicating that this phenotypic effect might be specific to *Puf3*-dependent mitochondrial genes only (Supporting Information S1: Figure S13C).

4 | DISCUSSION

Our work was based on the hypothesis that *MKT1* allele-mediated stress resistance relied on posttranscriptional modulation of mitochondrial activity via Puf3 targets. While establishing the individual roles of *PBP1* and *PUF3* as interacting genes, we attempted to provide mechanistic insights for these allelic interactions. From the tested environments ranging from oxidative, genotoxic, translational stress, cadmium chloride and high-temperature growth, we identified the diverse stress conditions where the wild-type M strain consistently grew better than the S strain (Figure 1 and Supporting Information S1: Figure S14).

Interestingly, Puf3 upregulated the expression of a few of its mitochondrial targets in stress conditions specific to the M strain, indicating the role of mitochondria in *MKT1* allele-specific stress resistance (Figure 4). A few of these mitochondrial target genes were observed to be crucial for the M strain exhibiting better fitness in diverse stress conditions. This difference in fitness was dependent on *PBP1* or *PUF3* or both in an environment-specific manner (Figures 5 and 6). This indicated that the role of the *MKT1* allele on fitness was both dependent on the environment and on the presence of *PBP1* and *PUF3*.

The formation of the Mkt1–Pbp1–Pab1 complex facilitates posttranscriptional regulation by Mkt1. The growth phenotype of the S strain was different from S-*pbp1Δ* in CYC and H_2O_2, indicating the formation of the Mkt1–Pbp1–Pab1 complex remains unaffected between M and S alleles under stress (Supporting Information S1: Figure S4). As Pbp1 localise to stress granules regulating transcript deadenylation (Swisher & Parker, 2010), this particular association allows Mkt1 to control the stress-specific stability of mRNA. Mkt1, with its uncharacterised interaction with Puf3, was observed regulating Puf3 target degradation in an allele-specific manner. Puf3, while binding to its target mRNA, governed their access to translation machinery and was known to transiently repress nuclear-encoded mitochondrial transcripts in oxidative stress (Rowe et al., 2014). Our analysis with Puf3 target deletion strains in diverse environments confirmed that the allele-specific phenotype of *MKT1* was both Pbp1 and Puf3 dependent. This indicates that the ability of the M allele to stabilise stress-specific mitochondrial transcripts to modulate mitochondrial activity accounts for its better stress responses than the S allele. However, the nature of the interaction between the $MKT1^{89G}$–Pbp1–Pab1 complex and Puf3 to specify the fate of a transcript is unknown. From our results, it is evident that Mkt1–Pbp1–Pab1 complex formation is independent of the *MKT1* allelic background and the environment. However, the higher expression level of a few Puf3 target genes in the M strain indicates that the interaction of the Mkt1–Pbp1–Pab1 complex with Puf3 might be restricted to the $MKT1^{89G}$ allele (Figure 3a).

The possible mechanisms by which the Puf target transcript can be regulated include interactions from other Puf proteins exemplified in *ZEO1* mRNA interacting with both Puf1 and Puf2 (Haramati et al., 2017), facilitating mRNA degradation by promoting deadenylation (Olivas, 2000) and mRNA localisation to mitochondria via Mdm12 and Tom20 (Miller et al., 2014).

Our growth experiments have established the qualitative effect of the M-allele's growth advantage compared to the S-allele across multiple stress conditions in wild type and most of the Puf3 target deletion backgrounds (Figures 5 and 6). However, the magnitude of growth advantage, that is, the difference between the fitness of M and S backgrounds, was variable with respect to each deletion across the environments (Supporting Information S1: Figure S15). For example, the effect of deletion of these mitochondrial genes *COX17*, *MRS1* and *RDL2* was variable with respect to the environment and the allelic background. The influence of these genes on the

growth difference between the M and the S strains was higher in H_2O_2 compared to CYC and 4NQO. One of the interesting observations was that *IVY1*, as a nonmitochondrial Puf3 target, had a phenotype similar to the wild type in H_2O_2.

Our results highlight another level of regulatory complexity where coding polymorphisms in QTL, like *MKT1*, can modulate multiple stress responses through posttranscriptional control in an environment-specific manner.

AUTHOR CONTRIBUTIONS

Koppisetty Viswa Chaithanya and Himanshu Sinha designed all the experiments and wrote the manuscript. Koppisetty Viswa Chaithanya performed all the experiments.

ACKNOWLEDGEMENTS

The authors acknowledge help from Rajeeva Lokshanan in the statistical analysis of some of the data. The authors thank K. Subramanian for critically reading the manuscript and comments. K. V. C. acknowledges the University Grant Commission Junior Research Fellowship. H. S. acknowledges intramural funding from IIT Madras and Excelra Knowledge Solutions Pvt. Ltd. (CR/22-23/0026/BT/EXCE/008752).

CONFLICT OF INTEREST STATEMENT

The authors declare no conflict of interest.

DATA AVAILABILITY STATEMENT

The data that supports the findings of this study are available in the Supporting Information of this article.

ORCID

Koppisetty Viswa Chaithanya http://orcid.org/0009-0000-1181-2950

Himanshu Sinha http://orcid.org/0000-0001-7031-0491

REFERENCES

Buchan, J. R., & Parker, R. (2009). Eukaryotic stress granules: The ins and outs of translation. *Molecular Cell*, *36*(6), 932–941. https://doi.org/10.1016/j.molcel.2009.11.020

Buchan, J. R., Yoon, J. H., & Parker, R. (2011). Stress-specific composition, assembly and kinetics of stress granules in *Saccharomyces cerevisiae*. *Journal of Cell Science*, *124*(Pt 2), 228–239. https://doi.org/10.1242/jcs.078444

Causton, H. C., Ren, B., Koh, S. S., Harbison, C. T., Kanin, E., Jennings, E. G., Lee, T. I., True, H. L., Lander, E. S., & Young, R. A. (2001). Remodeling of yeast genome expression in response to environmental changes. *Molecular Biology of the Cell*, *12*(2), 323–337. https://doi.org/10.1091/mbc.12.2.323

Chow, G. C. (1960). Tests of equality between sets of coefficients in two linear regressions. *Econometrica*, *28*(3), 591. https://doi.org/10.2307/1910133

Costa, J. M., Alanio, A., Moukoury, S., Clairet, V., Debruyne, M., Poveda, J. D., & Bretagne, S. (2013). Direct genotyping of *Toxoplasma gondii* from amniotic fluids based on B1 gene polymorphism using minisequencing analysis. *BMC Infectious Diseases*, *13*(1), 552. https://doi.org/10.1186/1471-2334-13-552/FIGURES/2

Deutschbauer, A. M., & Davis, R. W. (2005). Quantitative trait loci mapped to single-nucleotide resolution in yeast. *Nature Genetics*, *37*(12), 1333–1340. https://doi.org/10.1038/ng1674

Dimitrov, L. N., Brem, R. B., Kruglyak, L., & Gottschling, D. E. (2009). Polymorphisms in multiple genes contribute to the spontaneous mitochondrial genome instability of *Saccharomyces cerevisiae* S288c strains. *Genetics*, *183*(1), 365–383. https://doi.org/10.1534/genetics.109.104497

Ehrenreich, I. M., Torabi, N., Jia, Y., Kent, J., Martis, S., Shapiro, J. A., Gresham, D., Caudy, A. A., & Kruglyak, L. (2010). Dissection of genetically complex traits with extremely large pools of yeast segregants. *Nature*, *464*(7291), 1039–1042. https://doi.org/10.1038/nature08923

Fazlollahi, M., Lee, E., Muroff, I., Lu, X. J., Gomez-Alcala, P., Causton, H. C., & Bussemaker, H. J. (2014). Harnessing natural sequence variation to dissect posttranscriptional regulatory networks in yeast. *G3: Genes|Genomes|Genetics*, *4*(8), 1539–1553. https://doi.org/10.1534/g3.114.012039

Foster, M. W., Forrester, M. T., & Stamler, J. S. (2009). A protein microarray-based analysis of S-nitrosylation. *Proceedings of the National Academy of Sciences of the United States of America*, *106*(45), 18948–18953. https://doi.org/10.1073/pnas.0900729106

Gampel, A., & Tzagoloff, A. (1989). Homology of aspartyl- and lysyl-tRNA synthetases. *Proceedings of the National Academy of Sciences of the United States of America*, *86*(16), 6023–6027. https://doi.org/10.1073/pnas.86.16.6023

García-Rodríguez, L. J., Gay, A. C., & Pon, L. A. (2007). Puf3p, a Pumilio family RNA binding protein, localizes to mitochondria and regulates mitochondrial biogenesis and motility in budding yeast. *The Journal of Cell Biology*, *176*(2), 197–207. https://doi.org/10.1083/jcb.200606054

Gasch, A. P., & Werner-Washburne, M. (2002). The genomics of yeast responses to environmental stress and starvation. *Functional & Integrative Genomics*, *2*(4–5), 181–192. https://doi.org/10.1007/s10142-002-0058-2

Genuth, N. R., & Barna, M. (2018). Heterogeneity and specialized functions of translation machinery: From genes to organisms. *Nature Reviews Genetics*, *19*(7), 431–452. https://doi.org/10.1038/S41576-018-0008-Z

Gerber, A. P., Herschlag, D., & Brown, P. O. (2004). Extensive association of functionally and cytotopically related mRNAs with Puf family RNA-binding proteins in yeast. *PLoS Biology*, *2*(3):e79. https://doi.org/10.1371/journal.pbio.0020079

Gietz, R. D., Schiestl, R. H., Willems, A. R., & Woods, R. A. (1995). Studies on the transformation of intact yeast cells by the LiAc/SS-DNA/PEG procedure. *Yeast*, *11*(4), 355–360. https://doi.org/10.1002/yea.320110408

Goldstein, A. L., & McCusker, J. H. (1999). Three new dominant drug resistance cassettes for gene disruption in *Saccharomyces cerevisiae*. *Yeast*, *15*(14), 1541–1553.

Gupta, I., Clauder-Münster, S., Klaus, B., Järvelin, A. I., Aiyar, R. S., Benes, V., Wilkening, S., Huber, W., Pelechano, V., & Steinmetz, L. M. (2014). Alternative polyadenylation diversifies post-transcriptional regulation by selective RNA–protein interactions. *Molecular Systems Biology*, *10*(2), 719. https://doi.org/10.1002/msb.135068

Gupta, S., Radhakrishnan, A., Raharja-Liu, P., Lin, G., Steinmetz, L. M., Gagneur, J., & Sinha, H. (2015). Temporal expression profiling identifies pathways mediating effect of causal variant on phenotype. *PLOS Genetics*, *11*(6), e1005195. https://doi.org/10.1371/journal.pgen.1005195

Haramati, O., Brodov, A., Yelin, I., Atir-Lande, A., Samra, N., & Arava, Y. (2017). Identification and characterization of roles for Puf1 and Puf2 proteins in the yeast response to high calcium. *Scientific Reports*, *7*(1), 3037. https://doi.org/10.1038/s41598-017-02873-z

Heaton, D., Nittis, T., Srinivasan, C., & Winge, D. R. (2000). Mutational analysis of the mitochondrial copper metallochaperone Cox17. *Journal of Biological Chemistry*, *275*(48), 37582–37587. https://doi.org/10.1074/jbc.M006639200

Janke, C., Magiera, M. M., Rathfelder, N., Taxis, C., Reber, S., Maekawa, H., Moreno-Borchart, A., Doenges, G., Schwob, E., Schiebel, E., & Knop, M. (2004). A versatile toolbox for PCR-based tagging of yeast genes: New fluorescent proteins, more markers and promoter substitution cassettes. *Yeast*, *21*(11), 947–962. https://doi.org/10.1002/YEA.1142

Kechavarzi, B., & Janga, S. (2014). Dissecting the expression landscape of RNA-binding proteins in human cancers. *Genome Biology*, *15*(1):R14. https://doi.org/10.1186/gb-2014-15-1-r14

Kreike, J., Schulze, M., Pillar, T., Körte, A., & Rödel, G. (1986). Cloning of a nuclear gene MRS1 involved in the excision of a single group I intron (bI3) from the mitochondrial COB transcript in *S. cerevisiae*. *Current Genetics*, *11*(3), 185–191. https://doi.org/10.1007/bf00420605

Lackner, D. H., Schmidt, M. W., Wu, S., Wolf, D. A., & Bahler, J. (2012). Regulation of transcriptome, translation, and proteome in response to environmental stress in fission yeast. *Genome Biology*, *13*(4):R25. https://doi.org/10.1186/gb-2012-13-4-r25

Lapointe, C. P., Preston, M. A., Wilinski, D., Saunders, H. A. J., Campbell, Z. T., & Wickens, M. (2017). Architecture and dynamics of overlapped RNA regulatory networks. *RNA*, *23*(11), 1636–1647. https://doi.org/10.1261/rna.062687.117

Lazar, T., Scheglmann, D., & Gallwitz, D. (2002). A novel phospholipid-binding protein from the yeast *Saccharomyces cerevisiae* with dual binding specificities for the transport GTPase Ypt7p and the Sec1-related Vps33p. *European Journal of Cell Biology*, *81*(12), 635–646. https://doi.org/10.1078/0171-9335-00290

Lee, S. I., Dudley, A. M., Drubin, D., Silver, P. A., Krogan, N. J., Pe'er, D., & Koller, D. (2009). Learning a prior on regulatory potential from eQTL data. *PLoS Genetics*, *5*(1), e1000358. https://doi.org/10.1371/journal.pgen.1000358

Liti, G., Carter, D. M., Moses, A. M., Warringer, J., Parts, L., James, S. A., Davey, R. P., Roberts, I. N., Burt, A., Koufopanou, V., Tsai, I. J., Bergman, C. M., Bensasson, D., O'Kelly, M. J. T., van Oudenaarden, A., Barton, D. B. H., Bailes, E., Nguyen, A. N., Jones, M., … Louis, E. J. (2009). Population genomics of domestic and wild yeasts. *Nature*, *458*(7236), 337–341. https://doi.org/10.1038/nature07743

Loll-Krippleber, R., & Brown, G. W. (2017). P-body proteins regulate transcriptional rewiring to promote DNA replication stress resistance. *Nature Communications*, *8*(1), 558. https://doi.org/10.1038/s41467-017-00632-2

Martínez-Salas, E., Lozano, G., Fernandez-Chamorro, J., Francisco-Velilla, R., Galan, A., & Diaz, R. (2013). RNA-binding proteins impacting on internal initiation of translation. *International Journal of Molecular Sciences*, *14*(11), 21705–21726. https://doi.org/10.3390/ijms141121705

Miller, M. A., Russo, J., Fischer, A. D., Lopez Leban, F. A., & Olivas, W. M. (2014). Carbon source-dependent alteration of Puf3p activity mediates rapid changes in the stabilities of mRNAs involved in mitochondrial function. *Nucleic Acids Research*, *42*(6), 3954–3970. https://doi.org/10.1093/nar/gkt1346

Morano, K. A., Grant, C. M., & Moye-Rowley, W. S. (2012). The response to heat shock and oxidative stress in *Saccharomyces cerevisiae*. *Genetics*, *190*(4), 1157–1195. https://doi.org/10.1534/genetics.111.128033

Olivas, W. (2000). The Puf3 protein is a transcript-specific regulator of mRNA degradation in yeast. *The EMBO Journal*, *19*(23), 6602–6611. https://doi.org/10.1093/emboj/19.23.6602

Pel, H. J., Maat, C., Rep, M., & Grivell, L. A. (1992). The yeast nuclear gene *MRF1* encodes a mitochondrial peptide chain release factor and cures several mitochondrial RNA splicing defects. *Nucleic Acids Research*, *20*(23), 6339–6346. https://doi.org/10.1093/nar/20.23.6339

Rowe, W., Kershaw, C. J., Castelli, L. M., Costello, J. L., Ashe, M. P., Grant, C. M., Sims, P. F. G., Pavitt, G. D., & Hubbard, S. J. (2014). Puf3p induces translational repression of genes linked to oxidative stress. *Nucleic Acids Research*, *42*(2), 1026–1041. https://doi.org/10.1093/nar/gkt948

Saint-Georges, Y., Garcia, M., Delaveau, T., Jourdren, L., Le Crom, S., Lemoine, S., Tanty, V., Devaux, F., & Jacq, C. (2008). Yeast mitochondrial biogenesis: A role for the PUF RNA-binding protein Puf3p in mRNA localization. *PLoS One*, *3*(6), e2293. https://doi.org/10.1371/journal.pone.0002293

Simpson, C. E., & Ashe, M. P. (2012). Adaptation to stress in yeast: To translate or not. *Biochemical Society Transactions*, *40*(4), 794–799. https://doi.org/10.1042/bst20120078

Sinha, H., David, L., Pascon, R. C., Clauder-Münster, S., Krishnakumar, S., Nguyen, M., Shi, G., Dean, J., Davis, R. W., Oefner, P. J., McCusker, J. H., & Steinmetz, L. M. (2008). Sequential elimination of major-effect contributors identifies additional quantitative trait loci conditioning high-temperature growth in yeast. *Genetics*, *180*(3), 1661–1670. https://doi.org/10.1534/genetics.108.092932

Smith, E. N., & Kruglyak, L. (2008). Gene–environment interaction in yeast gene expression. *PLoS Biology*, *6*(4), e83. https://doi.org/10.1371/journal.pbio.0060083

Steinmetz, L. M., Sinha, H., Richards, D. R., Spiegelman, J. I., Oefner, P. J., McCusker, J. H., & Davis, R. W. (2002). Dissecting the architecture of a quantitative trait locus in yeast. *Nature*, *416*(6878), 326–330. https://doi.org/10.1038/416326a

Sun, X., Wang, Z., Guo, X., Li, H., & Gu, Z. (2016). Coordinated evolution of transcriptional and post-transcriptional regulation for mitochondrial functions in yeast strains. *PLoS One*, *11*(4), e0153523. https://doi.org/10.1371/journal.pone.0153523

Swinnen, S., Schaerlaekens, K., Pais, T., Claesen, J., Hubmann, G., Yang, Y., Demeke, M., Foulquié-Moreno, M. R., Goovaerts, A., Souvereyns, K., Clement, L., Dumortier, F., & Thevelein, J. M. (2012). Identification of novel causative genes determining the complex trait of high ethanol tolerance in yeast using pooled-segregant whole-genome sequence analysis. *Genome Research*, *22*(5), 975–984. https://doi.org/10.1101/gr.131698.111

Swisher, K. D., & Parker, R. (2010). Localization to, and effects of Pbp1, Pbp4, Lsm12, Dhh1, and Pab1 on stress granules in *Saccharomyces cerevisiae*. *PLoS One*, *5*(4), e10006. https://doi.org/10.1371/journal.pone.0010006

Tadauchi, T., Inada, T., Matsumoto, K., & Irie, K. (2004). Posttranscriptional regulation of *HO* expression by the Mkt1–Pbp1 complex. *Molecular and Cellular Biology*, *24*(9), 3670–3681. https://doi.org/10.1128/MCB.24.9.3670-3681.2004

Wang, M., Ogé, L., Perez-Garcia, M. D., Hamama, L., & Sakr, S. (2018). The PUF protein family: Overview on PUF RNA targets, biological functions, and post transcriptional regulation. *International Journal of Molecular Sciences*, *19*(2), 410. https://doi.org/10.3390/ijms19020410

Wickner, R. B. (1987). MKT1, a nonessential *Saccharomyces cerevisiae* gene with a temperature-dependent effect on replication of M2 double-atranded RNA. *Journal of Bacteriology*, *169*(11), 4941–4945. https://doi.org/10.1128/JB.169.11.4941-4945.1987

SUPPORTING INFORMATION

Additional supporting information can be found online in the Supporting Information section at the end of this article.

How to cite this article: Chaithanya, K. V., & Sinha, H. (2023). *MKT1* alleles regulate stress responses through posttranscriptional modulation of Puf3 targets in budding yeast. *Yeast*, *40*, 616–627. https://doi.org/10.1002/yea.3908